Published in : Journal of Constructional Steel Research (2022), vol. 189, 107092, pp. 1–15
DOI: 10. 1016/j.jcsr.2021.107092
Status : Postprint (Author's version)

DESIGN RULES FOR EQUAL-LEG ANGLE MEMBERS SUBJECTED TO COMPRESSION AND BENDING

Marios-Zois Bezas [a,b,*], Jean-François Demonceau [a], Ioannis Vayas [b], Jean-Pierre Jaspart [a]

[a] *Steel and Composite Construction, UEE Research Unit, Liège University, Belgium* [b] *School of Civil Engineering, Institute of Steel Structures, National Technical University of Athens, Athens, Greece*
** Corresponding author at: Université de Liège, Départment ArGEnCo, Quartier Polytech 1, All´ee de la Découverte 9 B52/3, Liège 4000, Belgium.*
E-mail addresses: Marios-Zois.Bezas@uliege.be (M.-Z. Bezas), jfdemonceau@uliege.be (J.-F. Demonceau), vastahl@central.ntua.gr (I. Vayas), jean-pierre.jaspart@ uliege.be (J.-P. Jaspart).

Keywords: Angle cross-section Resistance, Stability of members Buckling, Numerical simulations, Eurocode 3

Abstract

Angle profiles are amongst the most common structural steel shapes for construction purposes. However, their specific features clearly discern them from other types of common sections, what inevitably leads to the need for the development of specific design provisions. In this paper, extensive numerical and experimental studies have been conducted to propose a complete and duly validated set of design rules for resistance and stability of angle members subjected to individual and combined internal normal forces and moments. The proposed rules are written in the format of Eurocode 3 to allow a direct inclusion in forthcoming drafts.

1. Introduction

Angle sections belong to the most common structural steel shapes used in construction due to their easy production, transportation, and ability to be connected. They are available as hot-rolled or cold-formed profiles, as equal or unequal sections depending on the relative length of their legs, in steel grades up to S460 and in sizes ranging from small to large (20 to 300 mm). The preferred bolted connection of one leg to gusset plates lead to a most advantageous application as truss or diaphragm members in structural applications such as telecommunication or power transmission towers.

The equal-leg angle members considered here exhibit some properties that clearly distinguish them from the doubly symmetric ones. More specifically, angles are (i) monosymmetrical sections, (ii) they are open profiles with very small section constants in both torsion and warping, (iii) their bending capacity and radius of gyration around the weak axis are substantially lower compared to those in respect to the strong axis, (iv) their legs are possibly susceptible to local buckling, (v) their plastic resistances are significantly higher than their elastic ones and finally, (vi) due to the eccentric connection in one leg, they are also subjected to bending when used as single members. The above-listed features

Published in : Journal of Constructional Steel Research (2022), vol. 189, 107092, pp. 1–15
DOI: 10. 1016/j.jcsr.2021.107092
Status : Postprint (Author's version)

confirm that the existing design rules for other mostly doubly symmetric types of sections cannot safely cover angle sections, what inevitably leads to the need for development of specific design provisions for angle sections. In the absence of unified consistent rules for angles, European specifications provide individual rules and recommendations in various parts of Eurocode 3. More specifically, EN 1993-1-1 [1] as well as the forthcoming new version named prEN 1993-1-1 [2] provides general design rules for angles, EN 1993-3-1 [3] gives rules for the buckling resistance of angles as members in towers when connected eccentrically with bolts in one leg, EN 1993-1-8 [4] provides rules for the resistance of the above connection configuration, while the buckling resistance of class-4 angle sections is determined by EN 1993-1-5 [5]. Another European specification, the CENELEC standard EN 50341-1 [6] covers overhead electrical lines, addressing specific problems linked to such applications and providing specific rules for the verification of lattice towers and their constituting parts. It has to be noted that, in this last document, the design methods for angle sections may diverge from the rules provided in the Eurocodes as discussed in Ref. [7]. Unlike the European Codes, American Codes have written down in a single document, AISC 2000 [8], all the rules related to the design of angles and in addition separate specifications for the design of transmission towers [9].
Extensive research has been carried out to study the behavior of angle sections. It covers hot-rolled and cold-formed profiles, equal and unequal sections, beams or columns subjected to various types of loading, as well as different connection conditions. Schillo et al. [10] examine the buckling resistance rules of rolled angles to European standards discussed before (i.e EN 1993-1, EN 1993-3, EN 50341-1), and compare them to test results and numerical investigations considering various types of initial imperfections. Kettler et al. [11] highlight the importance of the end support conditions in their numerical study of rolled angles loaded in compression through bolted connections in one leg and present comparisons with experimental results and provisions of European standards.

Nomenclature

Latin upper-case symbols

A	cross-sectional area
A_{eff}	effective area of a cross-section
C_u, C_v	equivalent uniform moment factors E modulus of elasticity
L	length (member length, span length etc.)
L_{cr}	buckling length
M_{cr}	elastic critical moment for LTB, based on the gross cross-sectional properties
$M_{u,Ed}$, $M_{v,Ed}$	design bending moment about u-u and v-v axis respectively
$M_{ult,u}$, $M_{ult,v}$	ultimate test resistance to bending of the cross-section about u-u and v-v axis, respectively
$M_{u,Rd}$, $M_{v,Rd}$	design value of the resistance to bending moment about u-u and v-v axis respectively
$N_{bu,Rd}$	design value of the buckling resistance about u-u axis of a member in compression
$N_{bv,Rd}$	design value of the buckling resistance about v-v axis of a member in compression
N_{cr}	elastic critical axial force for the relevant buckling mode based on the gross cross-sectional properties
$N_{cr,u}$, $N_{cr,v}$	elastic critical axial force for flexural buckling about u-u and v-v axis, respectively, based on the gross cross- section properties
N_{Ed}	design axial force
N_{ult}	ultimate test resistance to axial force of the cross-section
$W_{eff,u}$	effective section modulus for bending about u-u axis

Published in : Journal of Constructional Steel Research (2022), vol. 189, 107092, pp. 1–15
DOI: 10. 1016/j.jcsr.2021.107092
Status : Postprint (Author's version)

$W_{el,u}$	elastic section modulus for bending about u-u axis

Latin lower-case symbols

c	outstand flange width ($c = h-t-r$)
f_y	yield strength
h	width or depth of a cross-section
r	radius of root fillet
t	thickness of a cross-section

Greek upper-case symbols

Φ	value to determine the reduction factor χ for flexural buckling
Φ_{LT}	value to determine the reduction factor χ_{LT} for lateral torsional buckling *Greek lower-case symbols*
α	imperfection factor
α_{LT}	imperfection factor for lateral torsional buckling
γ_{M1}	partial factor for resistance of members to instability assessed by member checks that equals 1,0 as recommended by EN 1993-1-1
ε	material parameter depending on f_y, equals $\varepsilon = \sqrt{235 / f_y \left[\frac{N}{mm^2}\right]}$
$\bar{\lambda}, \bar{\lambda}_u, \bar{\lambda}_v$	relative slenderness for flexural buckling
$\bar{\lambda}_p$	relative plate slenderness for plate buckling
$\bar{\lambda}_{LT}$	relative slenderness for lateral torsional buckling
ξ	interaction factor depending on the cross-section class
ρ, ρ_u	reduction factor for plate buckling
χ_{LT}	reduction factor for lateral torsional buckling
χ_u, χ_v	reduction factor due to flexural buckling about u-u and v-v axis, respectively
ψ	ratio of end moments in a beam

Hussain et al. [12] provide an interaction equation in the plastic range for the stability design of angles subjected to compression and biaxial bending. Concerning the design of cold-formed angle members subjected to compression, a considerable amount of innovative research work carried by Dinis et al. [13–15], led to the proposal of novel and more rational design rules based on the Direct Strength Method (DSM). This design approach has been extended in Ref. [16] to hot-rolled sections, applicable to short-to-intermediate angle columns under ideal support conditions subjected to compression. Bezas et al. [17] report on experimental and numerical studies of large hot-rolled angle members made of high strength steel (HSS) and give an extended literature review on relevant experimental investigations on angles. Finally, extensive experimental investigations have been carried out by various authors [18–20]; more details are given in section 4.

In the frame of the European RFCS-supported project ANGELHY [21], existing European specifications on rolled equal angle sections were reviewed, extensive experimental, analytical and numerical studies have been conducted and a complete set of design rules covering all aspects of design have been developed and duly validated. They include cross-section classification, cross-section design to individual internal forces and moments, for all ranges of response (plastic, elastic- plastic or elastic including local buckling), as well as corresponding rules for member design. The proposed design rules have been included as Annex F in the latest version of prEN 1993-3 [22] that is the part of

Published in : Journal of Constructional Steel Research (2022), vol. 189, 107092, pp. 1–15
DOI: 10. 1016/j.jcsr.2021.107092
Status : Postprint (Author's version)

Eurocode 3 dealing with towers, masts and chimneys, and as prEN, is subjected to discussion. Other parts, especially the general part EN 1993-1-1, were progressed to a state that no more interventions were possible at the time the rules were made available. The classification system and design rules for the cross-section resistance are given by Bezas et al. in Ref. [23], while this paper presents the design rules and their justification and validation. Concerning the resistance and stability of members, serving thus as a background document to Annex F of Ref. [22]. The proposed design methods were validated by numerical investigations and experimental tests. The extensive numerical parametrical studies were performed with the full non-linear software ABAQUS considering geometrical and material non-linearities, as they are described in detail in section 3. Experimental results were considered from tests carried out both within the current research project, as well as during previous experimental investigations. Most tests on hot- rolled angle sections were performed with regard to applications in mast and towers. Consequently, the loading and support conditions in the tests imitate the actual ones as found in those applications that obviously do not correspond to ideal ones. These tests have been used, as done before in the relevant literature and by Code drafting panels in order to develop and calibrate Code rules. The important influence of the support conditions should be introduced in the relevant buckling lengths for which the relevant Codes make proposals, but are not the objective of this paper.

2. Design rules for angle members

In the following, formulae about the design resistance and stability of equal-leg angle members as derived during the ANGELHY project, are presented, discussed and compared with the Eurocode 3 provisions. In absence of the availability of analytical solutions for general application, they constitute Engineering approximations based on following considerations:

- they should correctly represent the mechanical behavior and failure modes of cross-sections and members;
- they should cover stability checks under combined loading conditions, including compression and bending;
- they should smoothly adapt to specific cases, such as individual loadings and failure modes;
- they should be closely connected to analytical expressions for simple cases;
- they should remain simple and not too much overloaded with additional factors as a result of a calibration procedure to allow transparency and easy "by hand" control checks;
- they should easily adapt to the format of the existing Eurocode 3 rules, especially those of prEN 1993-1-1 that are applicable for other types of cross-sections and do not cover rolled angles.

The notations for the material properties, safety factors and other symbols follow those given in EN 1993-1-1. Fig. 1 illustrates the notations for the geometrical properties, including the geometrical and the principal axes.

2.1. Buckling resistance to compression

The buckling design resistance for axial compression may be determined from:

$$N_{b,Rd} = \begin{cases} x_{min}\dfrac{Af_y}{\gamma_{M1}} & for\ class\ 1, 2\ and\ 3\ profiles \\ x_{min}\dfrac{A_{eff}f_y}{\gamma_{M1}} & for\ class\ 4\ profiles \end{cases} \quad (1)$$

where A_{eff} is the area of the effective cross-section that equals:

Published in : Journal of Constructional Steel Research (2022), vol. 189, 107092, pp. 1–15
DOI: 10. 1016/j.jcsr.2021.107092
Status : Postprint (Author's version)

$$A_{eff} = A - 2ct(1-\rho) \quad (2)$$

The reduction factor ρ for outstand plated elements due to local buckling is given in EN 1993–1-5 as below:

$$\rho = \begin{cases} 1{,}0 & for\ \bar{\lambda}_p \le 0{,}748 \\ \frac{\bar{\lambda}_p - 0{,}188}{\bar{\lambda}_p^2} & for\ \bar{\lambda}_p > 0{,}748 \end{cases} \quad (3)$$

considering the relative plate slenderness of legs equal to:

$$\bar{\lambda}_p = \sqrt{x_{min}}\,\frac{\frac{c}{t}}{18{,}6\varepsilon} \quad (4)$$

The buckling reduction factor χ_{min} is determined as a function of the relative slenderness $\bar{\lambda}$ of the compression member for the flexural buckling modes only:

$$X_{MIN} = \{X_U; X_V\} \quad (5)$$

The relative slenderness λ should be taken for all cross-section classes as:

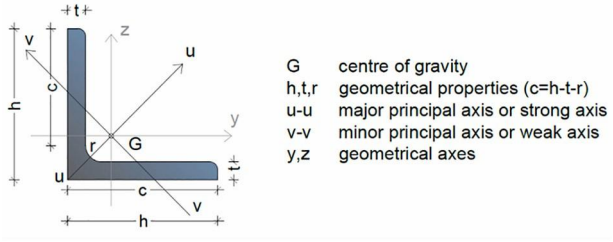

Fig. 1. Notations for geometrical properties.

$$\bar{\lambda} = \sqrt{\frac{Af_y}{N_{cr}}} \quad (6)$$

where N_{cr} is the minimum elastic critical force for the flexural buckling mode based on the gross cross-sectional properties and boundary conditions, i.e. $N_{cr} = \min\{N_{cr,u}; N_{cr,v}\}$.

The value of the buckling reduction factors χ_u, χ_v for the appropriate relative slenderness $\bar{\lambda}_u$, $\bar{\lambda}_v$ should be determined from buckling curve b for steel grades S235-S420, or buckling curve a for higher steel grades (≥S460).

It may be seen that the local plate slenderness $\bar{\lambda}_p$ (eq. 4), is made dependent by the proposed design rules not only on the geometric and material properties of the cross section (c/t-ratio and correspondingly ε), but also on the overall buckling reduction factor χ_{min}. This means that $\bar{\lambda}_p$ decreases, as the overall slenderness of the angle member increases. As a result, the proposed design rules, in line with Ref. [24], correctly account for the fact that, in concentrically compressed members, the effects of local buckling diminish as the length of the angle member, and the relevant global slenderness, increases.

Furthermore, it may be seen that, as mentioned in Ref. [25], the ultimate strength $N_{b,Rd}$ of concentrically compressed angle members is substantially influenced by the end support conditions. Indeed, the global slenderness $\bar{\lambda}$ and the relevant reduction factor χ_{min}, introduced in eq. 1, depend on the Euler critical buckling loads and therefore on the restraint that provide the support conditions. The authors work currently on the development of methods to define the restraint conditions provided by various end detail configurations, typical in telecommunication and transmission towers.

Published in : Journal of Constructional Steel Research (2022), vol. 189, 107092, pp. 1–15
DOI: 10. 1016/j.jcsr.2021.107092
Status : Postprint (Author's version)

2.1.1. Comparison with EN 1993-1-1 and prEN 1993-1-1 provisions

EN 1993-1-1, clause 6.3.1 recommends the use of buckling curve b whatever is the steel grade while, in the forthcoming new version of this normative document, prEN 1993-1-1, clause 8.3.1, curve b is still used for steel grades S235-S420 but curve a is proposed for higher steel grades (≥ S460). The proposed method adopts the same buckling curves as in the provisions of prEN 1993-1-1.

Additionally, both versions recommend to use the "elastic critical load for the relevant buckling mode" for the evaluation of the non- dimensional slenderness, i.e. the minimum eigenvalue amongst all flexural and flexural-torsional buckling modes. A pure torsional mode cannot be obtained for a centrally loaded angle column as explained in Ref. [26]. Through numerical studies on angles in compression (see section 3.2) exhibiting various profiles, lengths and steel grades, it is seen that weak axis flexural buckling always prevail at failure even for angles exhibiting a flexural-torsional elastic critical instability mode. Therefore, it seems reasonable to calculate the member resistance of rolled angles by using the slenderness for flexural buckling only and not by referring to the "relevant buckling mode" which includes torsional effects, as EN 1993-1-1, clause 6.3.1, and pr EN 1993-1-1, clause 8.3.1 prescribe.

The slenderness $\bar{\lambda}$ is determined by eq. 6 introducing for class-4 section the plastic axial force of the gross instead of the effective cross section that is used by EN 1993-1-1. This conservative assumption is counterbalanced by reducing the plate slenderness to define the effective cross-section by eq. 4 as shown later on.

Finally, the interaction between local and global buckling are considered in the definition of the relative plate slenderness $\bar{\lambda}_p$ via the term $\sqrt{x_{min}}$, unlike in EN 1993-1-1.

2.2. Lateral torsional buckling resistance to strong axis bending

The bending resistance of laterally unrestrained beams is determined by application of a reduction factor, accounting for effects of lateral torsional buckling, to the relevant resistance of the same beams assumed to be laterally restrained, as it is also recommended by the current provisions of Eurocode 3.

The bending resistance of laterally restrained beams is derived considering a linear transition between plastic and elastic bending resistances, as it is validated in Ref. [23], following the procedure for double symmetric cross-sections that was proposed by SEMI-COMP project [27]; according to SEMICOMP, a smooth transition between cross-section classes is allowed, removing thus any artificial stepwise prediction of resistance.

The design buckling resistance moment $M_{u,Rd}$ of a laterally unrestrained beam may accordingly be determined from:

$$M_{u,Rd} = \chi_{LT} W_u \frac{f_y}{\gamma_{M1}} \quad (7)$$

Where W_u is the section modulus about the u axis:

$$W_u = \alpha_{i,u} W_{el,u}, i = 2,3,4 \quad (8)$$

Where,

$$\alpha_{2,u} = 1{,}5 \; for \; class \; 1 \; or \; 2 \quad (9)$$

$$\alpha 3, u = \left[1 + \left(\frac{26{,}3\varepsilon - c/t}{26{,}3\varepsilon - 16\varepsilon}\right) \bullet (1{,}5 - 1)\right] \; for \; class \; 3 \quad (10)$$

$$\alpha_{4,u} = W_{eff,u} / W_{el,u} = \rho_u^2 \; for \; class \; 4 \quad (11)$$

Published in : Journal of Constructional Steel Research (2022), vol. 189, 107092, pp. 1–15
DOI: 10. 1016/j.jcsr.2021.107092
Status : Postprint (Author's version)

The reduction factor ρ_u for outstand plated elements due to local buckling can be evaluated through eq. 3, considering a reduced plate slenderness of the legs equal to:

$$\bar{\lambda}_p = \sqrt{\chi_{LT}}\ \frac{\frac{c}{t}}{35{,}58\varepsilon} \qquad (12)$$

The reduction factor for lateral torsional buckling χ_{LT} should be determined as a function of the relative slenderness $\overline{\lambda_{LT}}$ of the member:

$$\overline{\lambda_{LT}} = \sqrt{\frac{W_u f_y}{M_{cr}}} \qquad (13)$$

The elastic critical moment for lateral-torsional buckling M_{cr} is given by the following eq. 14 given in Ref. [8], with use of Table 1:

$$M_{cr} = C_b\ \frac{0{,}46 \bullet E \bullet h^2 \bullet t^2}{L} \qquad (14)$$

The value of the buckling reduction factor χ_{LT} for the relative slenderness $\overline{\lambda_{LT}}$ should be derived from buckling curve a, which can be determined by the eq. (6.57) of EN 1993-1-1: section 6.3.2.3 (1) for lateral-torsional buckling, using $\bar{\lambda}_{LT,0} = 0{,}4$ and $\beta = 1{,}00$ (see eq. 15 and eq. 16).

$$\chi_{LT} = \frac{1}{\phi_{LT} + \sqrt{\phi_{LT}^2 - \bar{\lambda}_{LT}^2}} \text{ but } \begin{cases} \chi_{LT} \leq 1{,}0 \\ \chi_{LT} \leq 1 \,/\, \bar{\lambda}_{LT}^2 \end{cases} \qquad (15)$$

$$\phi_{LT} = 0{,}5\left[1 + a_{LT}\left(\bar{\lambda}_{LT} - 0{,}4\right) + \bar{\lambda}_{LT}^2\right] \qquad (16)$$

Table 1
Determination of the C_b-factor for LTB [8].

General case:

$$C_b = \frac{12{,}5 M_{max}}{2{,}5 M_{max} + 3M_A + 4M_B + 3M_c} \leq 1{,}5$$

For linear moment distribution:

$$C_b = \frac{12{,}5}{7{,}5 + 5\psi} with\ -1 \leq \psi = \frac{M_2}{M_1} \leq 1$$

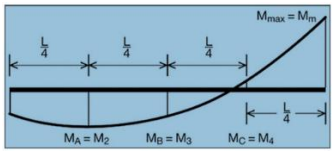

However, following in essence the limitations of EN 1993-1-1, lateral torsional buckling may be ignored ($\chi_{LT} = 1{,}0$) when one of the following conditions apply:

- $\bar{\lambda}_{LT} \leq \bar{\lambda}_{LT,0} (where\ \bar{\lambda}_{LT,0} = 0{,}4)$
- $\frac{M_{u,Ed}}{M_{cr}} = \bar{\lambda}_{LT,0}^{\ 2}$

2.2.1. Comparison with EN 1993-1-1 and prEN 1993-1-1

The lateral torsional buckling resistance is in line with EN 1993-1-1, clause 6.3.2, eq. (6.55) or prEN 1993-1-1, clause 8.3.2, eq. (8.79). However, like in flexural buckling, the interaction between local and global buckling are considered in the relative plate slenderness $\bar{\lambda}_p$ and not in the global slenderness $\bar{\lambda}_{LT}$. Buckling curve d is recommended by both

Published in : Journal of Constructional Steel Research (2022), vol. 189, 107092, pp. 1–15
DOI: 10. 1016/j.jcsr.2021.107092
Status : Postprint (Author's version)

normative documents while, a is adopted in the proposal as a result of the validation procedure based on numerical studies (see section 3.3).

The transition between elastic and plastic bending resistances adopts the proposals of SEMICOMP in contrast with the existing version of Eurocode 3, but in line with the forthcoming one, at least for doubly symmetric sections.

2.3. Resistance to weak axis bending

The cross-section resistance of angles subjected to weak axis bending depend on whether the tip is in tension or in compression, but not on the member length. Therefore, the member resistance coincides with the cross-section resistance as provided in Ref. [23].

2.4. Buckling resistance to bending and axial compression

The proposal check requires to fulfil two conditions for buckling around one or the other principal axis for angle members subjected to compression and biaxial bending. Torsional buckling is not checked separately but is included in the local buckling check.

- strong axis check

$$\left(\frac{N_{Ed}}{N_{bu,Rd}} + k_{vu}\frac{M_{u,Ed}}{M_{u,Rd}}\right)^{\xi} + K_{uv}\frac{M_{v,Ed}}{M_{v,Rd}} \leq 1 \qquad (17)$$

- weak axis check

$$\left(\frac{N_{Ed}}{N_{bv,Rd}} + k_{vu}\frac{M_{u,Ed}}{M_{u,Rd}}\right)^{\xi} + K_{vv}\frac{M_{v,Ed}}{M_{v,Rd}} \leq 1 \qquad (18)$$

where k_{ij} are the interaction factors that are provided in Table 2.
The ξ-factor is expressing a plastic, intermediate of elastic interaction and may be determined accordingly as follows:

$$c\,/\,t \leq 16\varepsilon : \ \xi = 2 \qquad (19)$$

Table 2
Determination of k_{ij} factors.

k_{ij} factors	
$k_{uu} = \frac{c_u}{1-\frac{N_{ed}}{N_{cr,u}}}$	$k_{uv} = C_v$
$k_{vu} = C_u$	$k_{vv} = \frac{c_v}{1-\frac{N_{ed}}{N_{cr,v}}}$
$c_u = 0{,}6 + c_u = 0{,}6 + 0{,}4\Psi_u$	$c_v = 0{,}6 + 0{,}4\Psi_v$
$-1 \leq \Psi_u = \frac{M_{2u}}{M_{1u}}$	$-1 \leq \Psi_v = \frac{M_{2v}}{M_{1v}}$

$$16\varepsilon < c/t < 26{,}3\varepsilon : \ \xi = \left[1 + \left(\frac{26{,}3\varepsilon - \frac{c}{t}}{26{,}3\varepsilon - 16\varepsilon}\right)\right] \qquad (20)$$

$$c\,/\,t > 26{,}3\varepsilon : \ \xi = 1 \qquad (21)$$

Published in : Journal of Constructional Steel Research (2022), vol. 189, 107092, pp. 1–15
DOI: 10. 1016/j.jcsr.2021.107092
Status : Postprint (Author's version)

Obviously, in the vast majority of cases the weak axis check (i.e. eq. 18) dominates, given the big difference of the angle radii of gyration between the two principal axes. This is true, unless the bracing conditions are such that the member is practically restrained in respect to weak axis buckling, or the load eccentricity that results a bending moment $M_{u,Ed}$ around the strong axis is very large.

2.4.1. Comparison with EN 1993-1-1 and prEN 1993-1-1

The procedure exhibits similarities, but also differences with EN 1993-1-1, clause 6.3.3 and prEN 1993-1-1, clause 8.3.3. In both procedures there are two equations, respectively for buckling around one and the other principal axis, the equations have three terms (one for compression, two for bending around the principal axes), lateral torsional buckling is included in the strong axis bending term while local buckling is included through the properties of the effective section.

In contrast, in the proposed check, the factor ξ provided by eq. 19 to eq. 21, is introduced that makes the interaction between the three terms to look as non-linear. Of course, it has to be pointed out that the interaction relations in EN 1993-1-1 and prEN 1993-1-1 are also non-linear, despite they appear as linear. The quadratic term with $\xi = 2$, given by eq. 19, tries to cover the cross-section resistance check of class-2 cross-sections as derived in Vayas et al. [28], while $\xi = 1$ leads to a linear interaction as foreseen in elastic design. Furthermore, simpler expressions for the terms C_i and k_{ij}, but derived straightforward from the stability theory, are proposed. In fact, the terms k_{ij} represent the magnification factors of bending moments for simply supported members subjected to compression forces and end moments as derived by 2nd order elastic analysis, while the terms C_i represent the influence of a moment gradient along the member.

2.5. General method for angle sections

The general method proposed in EN 1993-1-1, clause 6.3.4 and prEN 1993-1-1, clause 8.3.4 for the evaluation of the stability of structural members or parts of structures applies to lateral and lateral torsional buckling for structural components with mono symmetric cross-sections, built-up or not, uniform or not, with complex support conditions or not, which are subject to compression and/or uni-axial bending in the plane, but which do not contain rotative plastic hinges.
The authors suggest applying it as follows for members with equal leg angles. The out-of-plane buckling resistance of the member is checked if the following equation applies: *a*

$$x_{op} \cdot \frac{a_{ult,k}}{\gamma_{M1}} \geq 1{,}0 \qquad (22)$$

where,

χ_{op} is the reduction factor corresponding to the non-dimensional slenderness $\bar{\lambda}_{op}$ and aimed at accounting for weak axis buckling only, as this is the predominate failure mode for angles. The selection of the buckling curve is based on Ref. [2].
$a_{ult,k}$ is the minimum load amplifier of the design loads to reach the characteristic value of elastic resistance of the most critical cross-section of the structural component considering its in plane behavior without taking lateral or lateral torsional buckling into account, but however accounting for all effects due to in plane geometrical deformation and imperfections, global and local, where relevant. It can be derived from the following equation:

Published in : Journal of Constructional Steel Research (2022), vol. 189, 107092, pp. 1–15
DOI: 10. 1016/j.jcsr.2021.107092
Status : Postprint (Author's version)

$$\alpha_{ult,k} \cdot \sigma_{max} = f_y \quad (23)$$

where σ_{max} is the maximum elastic stress in the most loaded section along the member length, defined as the sum of four terms:

$$\sigma_{max} = \sigma_N + \sigma_{e0} + \sigma_{Mu} + \sigma_{Mv} \quad (24)$$

In this one:

- the first term (σ_N) relates to the pure compression stress under the N_{Ed} force;
- the second term (σ_{e0}), to the second order maximum stress resulting from the amplification of the first order moment $N_{Ed} \cdot e_{0,EC3}$ ($e_{0,EC3}$ is in-plane equivalent imperfection as defined in Ref. [2]), i.e. the moment $N_{Ed} \cdot e_{0,EC3}[1/(1-N_{Ed}/N_{cr,u})]$;
- the third one (σ_{Mu}), relates to the second order maximum stress resulting from the amplification of the first order moment $N_{Ed} \cdot e_v$ (e_v is the in-plane load eccentricity), which can be estimated as $N\text{Ed} \cdot ev[1/(1-N\text{Ed}/N\text{cr,u})]$;
- the fourth term (σ_{Mv}) relates to the first order bending moment $N_{Ed} \cdot e_u$ (e_u is the out-of-plane load eccentricity).

The global relative slenderness $\overline{\lambda_{op}}$ for the structural component should be determined from the equation below, in which the term $\alpha_{cr,op}$ is the minimum load amplifier for the design loads to reach the elastic critical load of the structural component associated to weak axis buckling ($\alpha_{cr,op} = \alpha_{cr,v}$).

$$\overline{\lambda_{op}} = \sqrt{\frac{\alpha_{ult,k}}{\alpha_{cr,op}}} \quad (25)$$

In case that the angle is connected by the leg, the "in-plane" instability effects may be considered as negligible, 2nd order effects may be disregarded ($1/(1 - N_{Ed}/N_{cr,u}) = 1$) and e_0 may be taken equal to zero (in recognition of the rather limited impact of this parameter, as a result of the significant difference of the elastic critical loads for the *u* and *v* buckling axes respectively).
The cross-section resistance in bending may be evaluated by using eq.8. Conservatively, the elastic cross-section resistance (W_{el}) may be also used.

2.5.1. Comparison with EN 1993-1-1 and prEN 1993-1-1

The difference with the present and forthcoming code versions (Ref. [1] and Ref. [2]) lies in the definition of the reduction factor which aims to take into account only the weak axis buckling (instead of lateral and lateral torsional buckling. The term $\alpha_{cr,op}$ is therefore adapted accordingly.

3. Numerical validation

The validation of the proposed formulae for the prediction of the carrying capacity of members with equal leg angle sections is based on comparisons with the results of numerical simulations of the member response for a wide range of parameters. The profile sizes, the member lengths and the steel grades of the samples have been selected in order to collect a large number of samples with properties that are commonly used in steel towers (see Table 3). However, this is not limiting the range of application of the rules, as the parameters of the selected numerical samples shows

Published in : Journal of Constructional Steel Research (2022), vol. 189, 107092, pp. 1–15
DOI: 10. 1016/j.jcsr.2021.107092
Status : Postprint (Author's version)

that they can be easily used in other types of structures too. It has to be mentioned that the classification system used hereafter, is the one proposed in Ref [23].

Table 3
Cross-sections that commonly used in steel lattice towers.

Chords							
Cross-section	Use	Legth [m]	Steel grade	Cross-section	Use	Legth [m]	Steel grade
L70x70xt	Smallest cross-section for upper levels	1,0-2,0	S355 S460	L80x80xt	For low levels	1,0-2,0	S355 S460
L150x150xt	Standard cross-section	2,0-3,0	S355 S460	L70x70xt	For middle levels	1,0-2,0	S355 S460
L250x250xt	For high pylons at low levels	2,0-3,0	S355 S460	L45x45xt	For upper levels	1,0-2,0	S355 S460

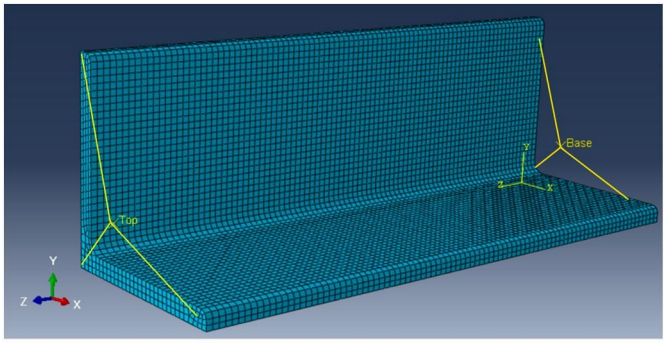

Fig. 2. Sample of the 3-D model used for the numerical analyses.

3.1. Description of the numerical models

The numerical models have been performed with ABAQUS [29] finite element software. The samples have been modelled as pin-ended with at least three volume linear elements over the thickness (see Fig. 2). The selection of the elements (linear instead of quadratic) does not influence the results. A denser mesh (i.e four volume elements per thickness) gives better results by 1–2%, but increases substantially the required time of the analysis, that is not desirable in combination with the high number of the numerical analyses to be performed. Although the end plates at the extremities of the samples have not been simulated, they have been considered indirectly through a specific constraint, so as to distribute uniformly the external applied loads but also to avoid any local failure at the point of application of the load. It has been shown in Ref. [30] that a considerable strength increase is observed when the secondary warping is prevented at the extremities of equal-leg cold- formed angle members. However, a similar effect has not been reported for hot-rolled angle sections.

Published in : Journal of Constructional Steel Research (2022), vol. 189, 107092, pp. 1–15
DOI: 10. 1016/j.jcsr.2021.107092
Status : Postprint (Author's version)

The finite element analyses were performed considering:

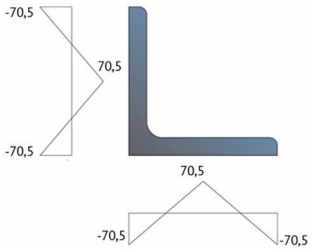

Fig. 3. Assumed distribution pattern of residual stresses in MPa based on Ref. [33–34].

- An initial bow imperfection of magnitude approximately equal to L [mm]/1000 with a deformation shape similar to the first member instability mode. This value combines the recommendation of the European norm EN 1090-2 [31], which prescribes that the deviation from straightness should be $\Delta \leq L$[mm]/750, with the provisions of prEN 1993-1-14 [32], which state that 80% of the geometric fabrication tolerances given in Ref. [31] should be applied. The direction of the imperfection has been implemented to lead the tip in compression.
- Residual stresses resulting from the hot-rolling procedure. The selected pattern (Fig. 3) is chosen from previous studies [33–34] in which appropriate measurements had been realized. It was shown that the residual stresses in hot rolled steel angle sections are independent of the steel grade and therefore a magnitude of $0{,}3 \cdot f_y$, that is approximately equal to 70 MPa for steel grade S235, is used.

Residual stresses in ABAQUS software may be implemented (i) by creating a sub-routine code so that the software is introducing them automatically, but the authors are not familiar to that, or (ii) by introducing an initial stress distribution. The latter requires to make the equilibrium of the stresses at the root of the angle section by hand, which is not desirable if considering the large number of analyses to be performed. Therefore, it has been decided to use an equivalent imperfection e_0 that will represent the effect of the combined action of both residual stresses and initial imperfections. To calibrate the value of the equivalent imperfection e_0, a few analyses have been performed with FINELG [35] finite element software, using beam elements. The angle members were considered as pin-ended with fictitious end plates at the extremities. The selection of the software has been done due to its easy and automatic way of introducing residual stresses in the model. The profiles and the material and geometrical properties of the tested samples are shown in Table 4.

First, a full non-linear analysis considering an initial imperfection (L/ 1000), an elastic perfectly plastic material law, as well as residual stresses (using the pattern shown in Fig. 3) has been performed for each one of the 10 different samples provided in Table 4 and the ultimate resistance $N_{ult,lm,ge+ma}$ has been reported. By introducing this value ($N_{ult,lm,ge+ma}$) in eq. 26, a rough estimation of the equivalent imperfection e_0 can be found equal to $e_0 = L$[mm]/700 (initial calculated mean value L/757).

$$\sigma_{max} = \frac{N_{ult}}{A} + \frac{N_{ult} e_0}{\left(1 - \frac{N_{ult}}{N_{cr,v}}\right) W_v} = f_y \qquad (26)$$

Then a second full non-linear analysis, considering this time the equivalent imperfection (L/700) and an elastic perfectly plastic material law has been performed for each one of the 10 samples and the ultimate resistance $N_{ult,lm,eq}$ has been recorded and presented in Table 4. The mean value of the ratio $N_{ult,lm,ge+ma}/N_{ult,lm,eq}$ is equal to 0,99 with a COV of 2,0%.

Published in : Journal of Constructional Steel Research (2022), vol. 189, 107092, pp. 1–15
DOI: 10. 1016/j.jcsr.2021.107092
Status : Postprint (Author's version)

Finally, a third full non-linear analysis, considering the equivalent imperfection (L/700) has been performed with ABAQUS using solid elements. The mean value of the ratio $N_{ult,abaqus}/N_{ult,lm,ge+ma}$ is equal to 0,96 with a COV of 3,3%, which can be acceptable considering the different types of finite elements used in the two models (beam elements in FINELG and solid element in ABAQUS). Therefore, the equivalent imperfection $e_0 = L$[mm]/700 accounting for both geometric imperfections and residual stresses is finally used in the analyses performed with ABAQUS to validate the member resistance formulae.

3.2. Members in axial compression

The profiles, lengths and steel grades have been selected from Table 3, but the thicknesses have been chosen so as to have samples of different classes (class 1 and 4) and different buckling modes as flexural or flexural-torsional. The details are summarized in Table 5, including

Table 4
Details and results from FINELG concerning the analyses to determine the equivalent imperfection e_0.

No	Cross-Section	Length L [mm]	Steel grade	e_0 [mm] from eq. 26	$e_0 = L/700$ [mm]	$N_{ult,lm,ge+ma}$ [kN]	$N_{ult,lm,eq}$ [kN]	$N_{ult,lm,ge+ma}/N_{ult,lm,eq}$ [–]
1	L70 × 70 × 5	1000	S355	1,34	1,42	182,41	188,45	0,97
2	L70 × 70 × 5	1000	S460	1,26	1,42	217,71	216,77	1,00
3	L70 × 70 × 5	2000	S355	2,69	2,86	64,04	64,77	0,99
4	L70 × 70 × 5	2000	S460	2,52	2,86	64,61	65,62	0,98
5	L80 × 80 × 8	2000	S355	2,74	2,86	144,31	142,03	1,02
6	L80 × 80 × 8	2000	S460	2,58	2,86	148,54	146,35	1,01
7	L150 × 150 × 13	2000	S355	2,89	2,86	1029,72	1077,83	0,96
8	L150 × 150 × 13	2000	S460	2,73	2,86	1259,42	1267,67	0,99
9	L250 × 250 × 20	2000	S355	2,87	2,86	3156,6	3236,49	0,98
10	L250 × 250 × 20	2000	S460	2,67	2,86	4005,27	3939,71	1,02

also the ratio between the elastic critical load for flexural-torsional buckling and the minimum one obtained for flexural buckling.

The samples have been modelled as explained in section 3.1. However, for those where the first elastic eigenmode is a flexural-torsional one, three cases were considered in terms of initial imperfections:

a. equivalent imperfection $e_{0,FT} = L$[mm]/700 with a deformation shape similar to the first member instability mode, i.e. the flexural- torsional one as it is shown in Fig. 4(b), (c) (which correspond to $N_{ult(a)}$);

b. equivalent imperfection $e_{0,F} = L$[mm]/700 with a deformation similar to the first flexural instability mode as t is shown in Fig. 4(a) (which correspond to $N_{ult(b)}$);

Published in : Journal of Constructional Steel Research (2022), vol. 189, 107092, pp. 1–15
DOI: 10. 1016/j.jcsr.2021.107092
Status : Postprint (Author's version)

Table 5
Details for the samples subjected to a uniform compression load

No	Cross-Section	L [mm]	f_y [N/mm²]	Class	Eigenmode deformed shape	$N_{cr,FT/min}N_{cr,F}$ [–]
1	L70 × 70 × 5	1000	355	1	Flexural	1,05
2	L70 × 70 × 5	1000	460	4	Flexural	1,05
3	L70 × 70 × 5	2000	355	1	Flexural	2,64
4	L70 × 70 × 5	2000	460	4	Flexural	2,64
5	L70 × 70 × 6	1000	355	1	Flexural	1,43
6	L70 × 70 × 6	1000	460	1	Flexural	1,43
7	L70 × 70 × 6	2000	355	1	Flexural	3,01
8	L70 × 70 × 6	2000	460	1	Flexural	3,01
9	L70 × 70 × 7	1000	355	1	Flexural	1,82
10	L70 × 70 × 7	1000	460	1	Flexural	1,82
11	L70 × 70 × 7	2000	355	1	Flexural	3,25
12	L70 × 70 × 7	2000	460	1	Flexural	3,25
13	L70 × 70 × 10	1000	355	1	Flexural	2,71
14	L70 × 70 × 10	1000	460	1	Flexural	2,71
15	L70 × 70 × 10	2000	355	1	Flexural	3,53
16	L70 × 70 × 10	2000	460	1	Flexural	3,53
17	L150 × 150 × 13	2000	355	1	Flexural	1,29
18	L150 × 150 × 13	2000	460	1	Flexural	1,29
19	L150 × 150 × 13	3000	355	1	Flexural	2,25
20	L1150 × 150 × 13	3000	460	1	Flexural	2,25
21	L150 × 150 × 14	2000	355	1	Flexural	1,46
22	L150 × 150 × 14	2000	460	1	Flexural	1,46
23	L150 × 150 × 14	3000	355	1	Flexural	2,44
24	L150 × 150 × 14	3000	460	1	Flexural	2,44
25	L150 × 150 × 15	2000	355	1	Flexural	1,63
26	L150 × 150 × 15	2000	460	1	Flexural	1,63
27	L150 × 150 × 15	3000	355	1	Flexural	2,61
28	L150 × 150 × 15	3000	460	1	Flexural	2,61
29	L150 × 150 × 18	2000	355	1	Flexural	2,11
30	L150 × 150 × 18	2000	460	1	Flexural	2,11
31	L150 × 150 × 18	3000	355	1	Flexural	2,98
32	L150 × 150 × 18	3000	460	1	Flexural	2,98
33	L150 × 150 × 18	2000	355	4	Flexural-torsional	0,32
34	L150 × 150 × 18	2000	460	4	Flexural-torsional	0,32
35	L250 × 250 × 17	3000	355	4	Flexural-torsional	0,69
36	L250 × 250 × 17	3000	460	4	Flexural-torsional	0,69
37	L250 × 250 × 20	2000	355	1	Flexural-torsional	0,45
38	L250 × 250 × 20	2000	460	4	Flexural-torsional	0,45
39	L250 × 250 × 20	3000	355	1	Flexural-torsional	0,99
40	L250 × 250 × 20	3000	460	4	Flexural-torsional	0,99
41	L250 × 250 × 22	2000	355	1	Flexural-torsional	0,54
42	L250 × 250 × 22	2000	460	1	Flexural-torsional	0,54
43	L250 × 250 × 22	3000	355	1	Flexural	1,11
44	L250 × 250 × 22	3000	460	1	Flexural	1,11
45	L250 × 250 × 26	2000	355	1	Flexural-torsional	0,75
46	L250 × 250 × 26	2000	460	1	Flexural-torsional	0,75
47	L250 × 250 × 26	3000	355	1	Flexural	1,48
48	L250 × 250 × 26	3000	460	1	Flexural	1,48

Published in : Journal of Constructional Steel Research (2022), vol. 189, 107092, pp. 1–15
DOI: 10. 1016/j.jcsr.2021.107092
Status : Postprint (Author's version)

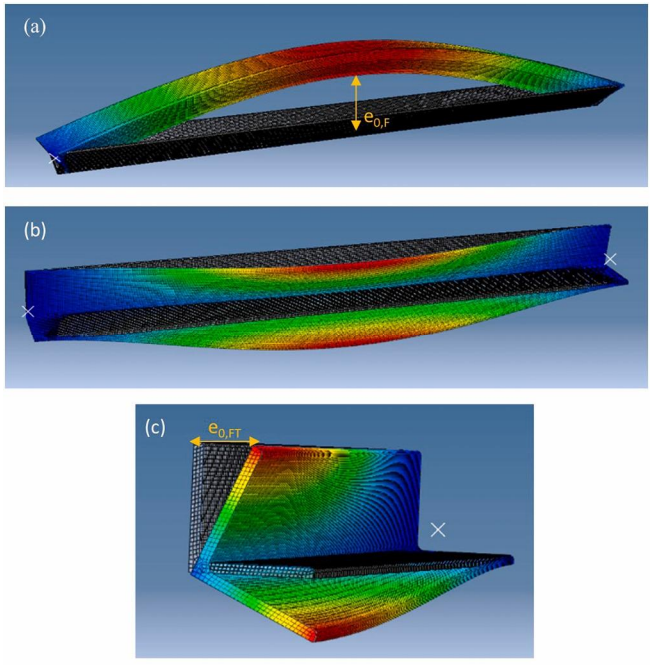

Fig. 4. Typical shape of the initial imperfection of a member with (a) flexural eigenmode and (b) flexural-tortional eigenmode; (c) middle cross-section of the member for case (b).

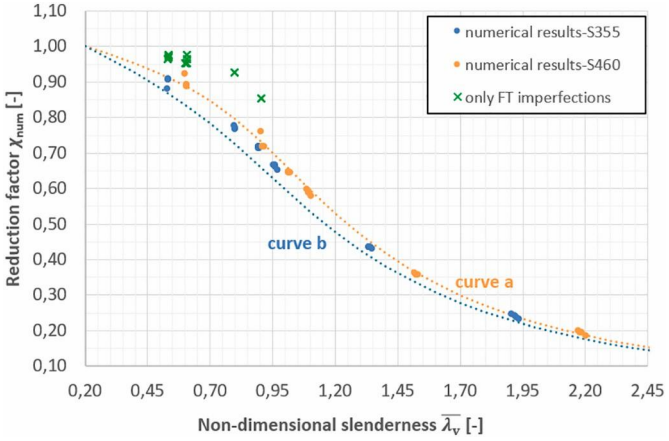

Fig. 5. Comparison of numerical results with buckling curves of prEN 1993–1-1.

c. equivalent imperfection $e_0 = e_{0,FT} + e_{0,F}$ (which correspond to $N_{ult\ (c)}$); $e_{0,FT} = L/700$ with a deformation shape similar to the first member instability mode (flexural-torsional) and $e_{0,F} = L/700$ with a deformation shape similar to the first flexural instability to counterbalance the fact that, in most of these cases, the torsional component predominates in the flexural-torsional mode. The combination of both modes is done automatically through the software.

For all the cases, the amplitude $e_0 = L$[mm]$/700$ is measured at the more distant node of the deformed shape (colourful) from the undeformed (grey) one, as illustrated in Fig. 4. Even though, in case c, there is (i) a twist of the cross-section and (ii) an initial flexural deflection a bit higher than in case b, the difference between the values $N_{ult(b)}$ and $N_{ult(c)}$ is negligible (less than 0,5%).

Published in : Journal of Constructional Steel Research (2022), vol. 189, 107092, pp. 1–15
DOI: 10. 1016/j.jcsr.2021.107092
Status : Postprint (Author's version)

Fig. 5 illustrates the numerical results compared with the reference buckling curves a and b as they are reported in [2]. The buckling reduction factor χ_{num} of the numerically tested samples has been evaluated as $\chi_{num} = N_{num}/N_{pl}$ and the slenderness using eq. 6. For the samples with a flexural-torsional eigenmode, two cases are distinguished in Fig. 5; the numerical results reported with blue/orange points have been evaluated using $N_{ult} = \min\{N_{ult(a)}, N_{ult(b)}, N_{ult(c)}\}$, while the results presented with green points using $N_{ult} = N_{ult(a)}$.
According to Ref. [1], the obtained numerical results for the S355 steel grade should be compared with curve b while for S460 with curve a. It can be easily observed that all the results referred to curve b are above the curve, while the results referred to curve a are in line, above or just a bit lower, which is acceptable given the 2% deviation that is considered. Regarding the results obtained using only an equivalent imperfection based on the 1st eigenmode (i.e. the flexural-torsional one), it is obvious that they are much higher even when compared with curve a. Through this comparison, it can be easily observed that the slenderness should be calculated using only the minimum elastic critical force for the flexural buckling mode as reported in section 2.1.

3.3. Members in strong axis bending

For this load case, the profiles, lengths and steel grades have been again selected from Table 3, while the thicknesses have been chosen to have samples of different classes (1 and 3). The details are summarized in Table 6. In order to study some more slender members, a few analyses have been additionally considered (marked with * in the table) with higher steel grades and member lengths. For each non-linear analysis, an initial imperfection of magnitude L[mm]/700 has been applied with a deformation shape similar to the first member instability mode to introduce a twist imperfection at the middle cross-section (see Fig. 6). It should be also noted that the application of eq. 14 was checked numerically with satisfactory results. Indeed, the mean value of the ratio $M_{cr,num}/M_{cr,anal}$ was equal to 0,989 with a COV of 4%.
Fig. 7 illustrates the numerical results compared with the buckling curves a and a_0 for LTB as they are defined by eq. (6.57) of EN 1993-1-1: §6.3.2.3. The reduction factor for lateral-torsional buckling $\chi_{LT,num}$ of the numerical samples has been evaluated by the equation $\chi_{LT,num} = M_{ult,u}/W_u f_y$ and the slenderness by using eq. 13.
It is seen in the graph that all the results are above curve a, while the most of them are below curve a_0; this validates the proposed buckling curve for LTB of angle sections. It can be also observed that the resistance of some class-3 profiles is above curve a_0. This could be explained by the fact that these cross-sections are classified as class 3 but with a $c/\varepsilon t$ ratio quite close to the class-2 limit, and so they are treated as class 3 sections while in reality, they reach their plastic resistance. On the contrary, due to the integration of the SEMICOMP aspects (where a smooth transition between cross-section classes 2 and 3 is allowed), a profile classified as Class 3, but very close to Class 2, should be characterized by a section resistance close to M_{pl}. To set this clear, one should have in mind that a profile with a $c/\varepsilon t$ approximately equal to 16, could have a ratio $M_{ult,u}/M_{pl}$ from 0,95 to 1,0. This justifies the small increased value of the numerical results. It should be also noticed that for higher $c/\varepsilon t$ ratios, the results conform to curve a.

3.4. Members in bending and axial compression

For the numerical studies, three cases have been considered in terms of bending moments: weak axis bending, strong axis bending and bi-axial bending, always in combination with an axial compression force. The results are presented in the following sub-sections.

Published in : Journal of Constructional Steel Research (2022), vol. 189, 107092, pp. 1–15
DOI: 10. 1016/j.jcsr.2021.107092
Status : Postprint (Author's version)

Table 6
Details for the samples subjected to a major axis bending moment.

No	Cross-Section	L [mm]	F_y [N/mm^2]	Class	No	Cross-Section	L [mm]	F_y [N/mm^2]	Class
1	L45 x 45 x 3	1000	355	1	29	L45 x 45 x 3	2000	355	1
2		1000	460	3	30		2000	460	3
3		2000	355	1	31		3000	355	1
4		2000	460	3	32		3000	460	3
5	L70 x 70 x 5	1000	355	1	33	L45 x 45 x 3	2000	355	1
6		1000	460	1	34		2000	460	1
7		2000	355	1	35		3000	355	1
8		2000	460	1	36		3000	460	1
9	L70 x 70 x 6	1000	355	1	37	L45 x 45 x 3	2000	355	1
10		1000	460	1	38		2000	460	1
11		2000	355	1	39		3000	355	1
12		2000	460	1	40		3000	460	1
13	L80 x 80 x 5	2000	355	1	41	L45 x 45 x 3	4000	355	1
14		2000	460	3	42		4000	460	1
15		3000	355	1	43		5000	355	1
16		3000	460	3	44		5000	460	1
17	L150 x 150 x 13	2000	355	1	45	L45 x 45 x 3	4000	550	1
18		2000	460	1	46		4000	690	3
19		3000	355	1	47		5000	55	1
20		3000	460	1	48		5000	690	3
21	L150 x 150 x 14	2000	355	1	49	L45 x 45 x 3	2000	355	1
22		2000	460	1	50		2000	460	1
23		3000	355	1	51		3000	355	1
24		3000	460	1	52		3000	460	1
25	L150 x 150 x 15	2000	355	1					
26		2000	460	1					
27		3000	355	1					
28		3000	460	1					

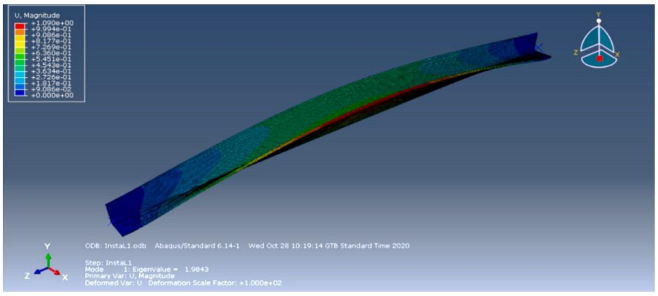

Fig. 6. Typical shape of initial imperfection for a member subjected to strong axis bending.

Published in : Journal of Constructional Steel Research (2022), vol. 189, 107092, pp. 1–15
DOI: 10. 1016/j.jcsr.2021.107092
Status : Postprint (Author's version)

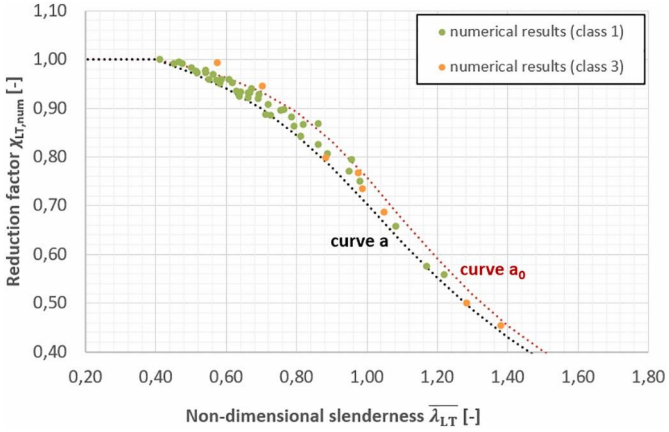

Fig. 7. Comparison of numerical results with buckling curves for LTB of EN 1993-1-1 [1].

3.4.1. Axial force and weak axis bending

The numerical investigations have been performed by considering only a constant weak axis moment along the member length caused by an eccentric axial force. The eccentricity lies on u-u axis (point P_1 in Fig. 8(a)), and ranges between 5 and 35 mm; the value has been chosen randomly for each sample. The details of the numerical samples are presented in Table 7. All the analyses are for the tip in compression, which is more critical than the tip in tension. Fig. 9 presents the ratio between numerical and analytical (section 2.4) resistance loads according to the weak axis slenderness $\overline{\lambda_v}$. The analytical load is determined as the maximum load that satisfies both eq. 17 and eq. 18, without safety factors. For all the samples, the weak axis check was the critical one, justifying the selection of $\overline{\lambda_v}$ in the abscissa. The test points represent besides the slenderness, different load eccentricities and, therefore, different contributions of the compression or bending terms to the design equations. Accordingly, different analytical- to-numerical ratios are achieved, for the same slenderness.

The mean value (m) of the ratio N_{num}/N_{anal} is equal to 1,03 with a standard deviation of 3,18%. There are only very few results where the analytical solution predicts lower values, with a maximal deviation of 3% in one test, while the (mean – s) value of all tests is close to 0,5%. This is completely acceptable, considering that strain hardening was neglected in the numerical analyses.

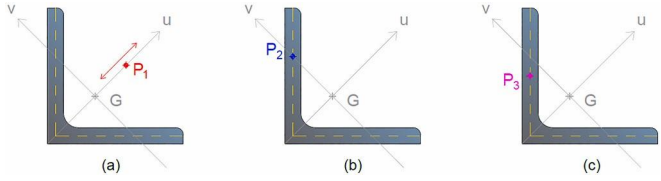

Fig. 8. Position of the load application point for the samples subjected to $N + M_v$ (b) $N + M_u$ (c) $N + M_u + M_v$.

Published in : Journal of Constructional Steel Research (2022), vol. 189, 107092, pp. 1–15
DOI: 10. 1016/j.jcsr.2021.107092
Status : Postprint (Author's version)

Table 7
Details for the samples subjected to an eccentric axial force causing a weak axis moment.

No	Cross-Section	L [mm]	F_y [N/mm²]	e_u [mm]	No	Cross-Section	L [mm]	F_y [N/mm²]	e_u [mm]
1	L45 x 45 x 3	1000	355	10	17	L150 x 150 x 14	2000	355	12
2		1000	460	10	18		2000	460	12
3		2000	355	10	19		3000	355	20
4		2000	460	10	20		3000	460	20
5		1000	355	5	21		2000	355	10
6	L70 x 70 x 5	1000	460	5	22	L150 x 150 x 18	2000	460	10
7		2000	355	20	23		3000	355	32
8		2000	460	20	24		3000	460	32
9		1000	355	35	25		2000	355	8
10	L70 x 70 x 6	1000	460	35	26	L250 x 250 x 17	2000	460	8
11		2000	355	35	27		3000	355	12
12		2000	460	35	28		3000	460	12
13		2000	355	25	29		2000	355	5
14	L80 x 80 x 5	2000	460	25	30	L250 x 250 x 22	2000	460	5
15		3000	355	25	31		3000	355	5
16		3000	460	25	32		3000	460	5

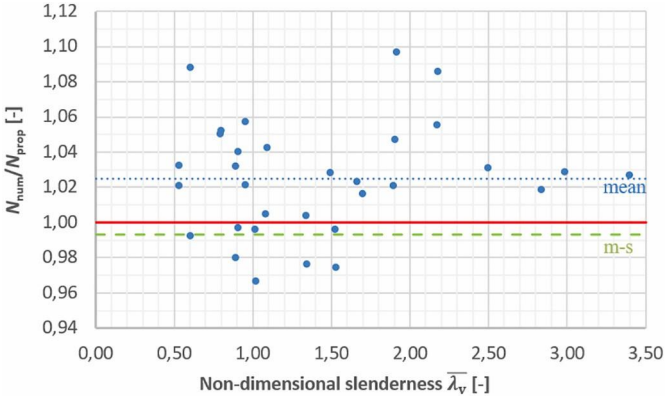

Fig. 9. Ratio between numerical and analytical loads for $N + M_v$.

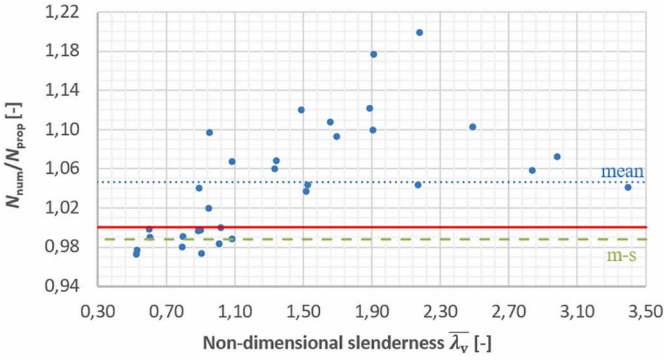

Fig. 10. Ratio between numerical and analytical loads for $N + M_u$

Published in : Journal of Constructional Steel Research (2022), vol. 189, 107092, pp. 1–15
DOI: 10. 1016/j.jcsr.2021.107092
Status : Postprint (Author's version)

3.4.2. Axial force and strong axis bending

The details (profiles/lengths/steel grades) of the numerical samples that have been used are the same than those presented in Table 7. The axial force is applied at the intersection point of the minor principal axis v-v with the middle line of the leg thickness (point P_2 in Fig. 8(b), which represents the case when the bolts can be placed on the v-axis) and ranges between 14,57 and 84,00 mm, depending on the profile geometry.

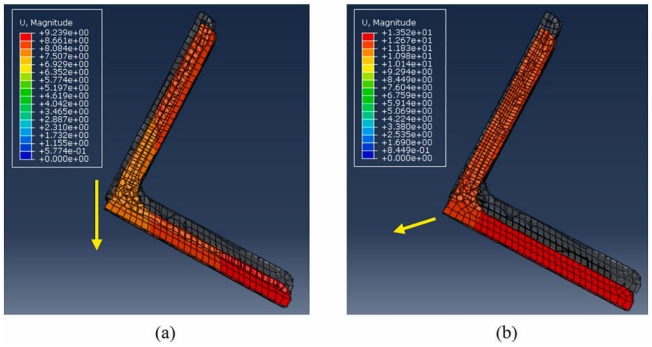

Fig. 11. Movement (indicated by the yellow arrow) of a profile subjected to an axial force and strong axis bending: (a) during initial loading steps and (b) at the failure load.

Fig. 10 presents the ratio between numerical load resistances and the analytical ones derived through the current proposal in accordance to the weak axis slenderness $\overline{\lambda_v}$. For all samples, weak axis check was again the critical one, as the member finally buckles along weak axis. This can be justified by the analytical approach, as lateral torsional-buckling is ignored (χ_{LT} = 1,0) due to one of the two conditions described in section 2.2; therefore, the member buckles only due to the axial load. Numerically, it can be shown from Fig. 11 that the member starts to move laterally (along strong axis) but finally buckles towards weak axis; the movements are indicating by the yellow arrows. This again justifies the tendency of angles to buckle along weak axis. The mean value of the ratio N_{num}/N_{anal} is equal to 1,05 with a standard deviation of 5,90%, and the validation of the analytical approach is effective if one accepts a 2% deviation from the numerical results.

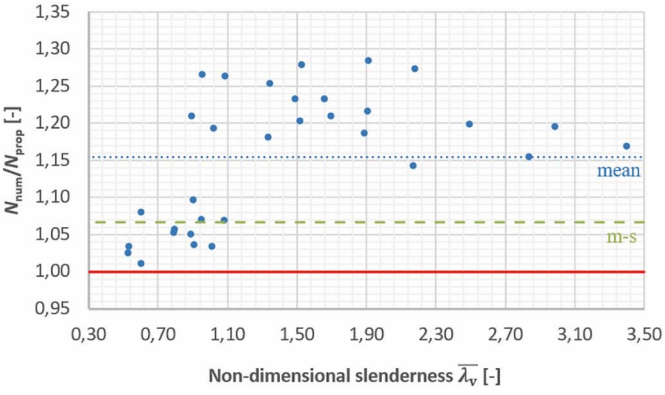

Fig. 12. Ratio between numerical and analytical loads for $N + M_u + M_v$.

3.4.3. Axial force and bi-axial bending

In this case, the axial force is applied on its mid-height of the leg on its mid-plane (point P_3 in Fig. 8(c)). This point could represent rather well the position of the connecting bolt for angles in structures. The details of the numerical samples that have been used, are the same as in the previous cases. Fig. 12 illustrates the ratio between numerical and

Published in : Journal of Constructional Steel Research (2022), vol. 189, 107092, pp. 1–15
DOI: 10. 1016/j.jcsr.2021.107092
Status : Postprint (Author's version)

analytical (section 2.4) resistance loads according to the weak axis slenderness $\overline{\lambda_v}$. The weak axis check was the critical one for this loading case too, and the member buckles towards weak axis.
The mean value of the ratio N_{num}/N_{anal} is equal to 1,15 with a standard deviation of 8,77%. It can be seen that the analytical approach for the combined resistance is validated through the numerical results.

3.5. General method for angle sections

The validation of the proposed general method in section 2.5 was done by referring to the numerical results in section 3.4.3. Therefore, the axial force is applied at the mid-height of the leg at the middle line of the leg thickness.
Three cases were considered, depending on the influence of some parameters, for investigation and validation:

- Case 1:

- "In-plane" 2nd order effects and bow imperfections are accounted for, in $a_{ult,k}$;
- e_0 is taken from prEN 1993-1-1:2019-§7.3.3.1 for relevant buckling curve (elastic verification);
- elastic cross-section resistance is used (W_{el}).

- Case 2:

- "In-plane" instability effects are considered as negligible;
- 2nd order effects are disregarded ($k_u = 1/(1-N_{Ed}/N_{cr,u}) = 1$) and e_0 is taken equal to zero (in recognition of the rather limited impact of this parameter); probably such an assumption should be limited to angles connected by one leg while, in this case, the strong axis moment remains limited, as its influence;
- - elastic cross-section resistance is used (W_{el}).

- Case 3:

- Same assumptions as in Case 2, but taking into account the actual cross-section resistance using $W_u = \alpha W_{el,u,}$.

Fig. 13 presents the ratio between numerical and analytical resistances obtained for the three different cases as a function of the weak axis slenderness $\overline{\lambda_v}$. The analytical resistance corresponds to the maximum load that satisfies eq. 22. Each case is represented by a colour and the relative horizontal line illustrates the mean value minus the standard deviation for each case.
It may be seen that the analytical approach for all the three cases is on the safe, with Case 1 to be the safest.

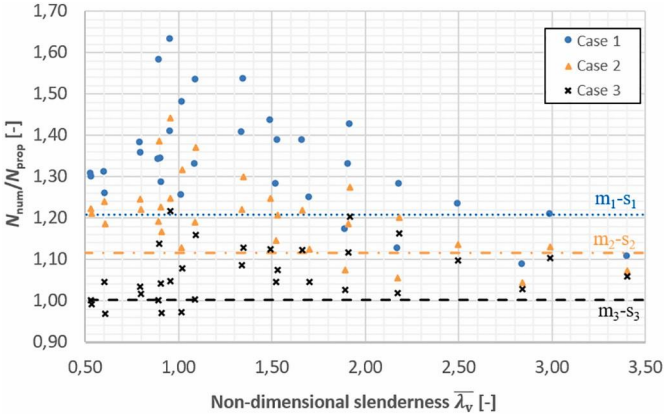

Fig. 13. Ratio between numerical loads and the analytical ones, obtained through the general method, for $N + M_u + M_v$.

Published in : Journal of Constructional Steel Research (2022), vol. 189, 107092, pp. 1–15
DOI: 10. 1016/j.jcsr.2021.107092
Status : Postprint (Author's version)

Case 3 is seen to be the closer to the reality. This results from the consideration of a higher cross-section resistance for class 1 and 2 cross-sections (in comparison to Case 1 and Case 2) and from a more reasonable assumption in terms of geometrical imperfection (in Case 1, e_0 is jointly applied in both planes: explicitly in the plane through the σ_{max} value and implicitly out-of-the-plane through the χ_{op} value).

4. Experimental validation

In the following, the design formulas given in section 2 are checked against tests that have been performed by various universities and are available in the literature. For all tests, the analytical load was determined using the actual geometrical and material properties without safety factors. A comparison with Eurocode 3 provisions is also reported.

4.1. Axial compression tests at Tsinghua University

At Tsinghua University, 66 tests were carried out on axially loaded columns from equal angle sections that were hinged at both extremities and reported in Ref. [18]. The cross-sections ranged from L 125x125x8 to L 200x200x14 and the material was high strength steel (HSS) S420. All the profiles were classified in class 4. For each section the nominal slenderness of the angle columns, defined as the ratio of the column length to the gyration radius of cross-section around the principal minor axis, were selected as approximately 30, 40, 50, 60 and 80. Although actual dimensions of the tested specimens have been measured, the authors are referring to the nominal slenderness so as to conform with the specimen labels used in Ref. [18].
Fig. 14 presents, for all tests, the ratio between the experimental resistances and the analytical ones obtained using current proposal (see section 2.1) according to the weak axis nominal slenderness λ_v. Fig. 15 presents the mean value (m) of the ratio between the experimental load resistances and the ones predicted by prEN 1993-1-1 and by the current proposal, as well as the mean minus one standard deviation value (m-s). There are only very few results where the analytical solution predicts lower values, with a maximal deviation of 5% in two tests, while the (mean – s) value of all tests with nominal slenderness 30 and 40 is 0,8% and 3,2% respectively. This is completely acceptable, considering again that strain hardening was neglected in the numerical analyses. It may be also seen that the current proposal gives a better prediction for the column capacity compared to the Eurocode 3. The conservative character of prEN 1993-1-1 may be explained by the fact that the non- dimensional slenderness is determined from the relevant buckling mode (in this experimental campaign the most were flexural-torsional ones), while as proposed, they should be based only on the flexural mode.

Published in : Journal of Constructional Steel Research (2022), vol. 189, 107092, pp. 1–15
DOI: 10. 1016/j.jcsr.2021.107092
Status : Postprint (Author's version)

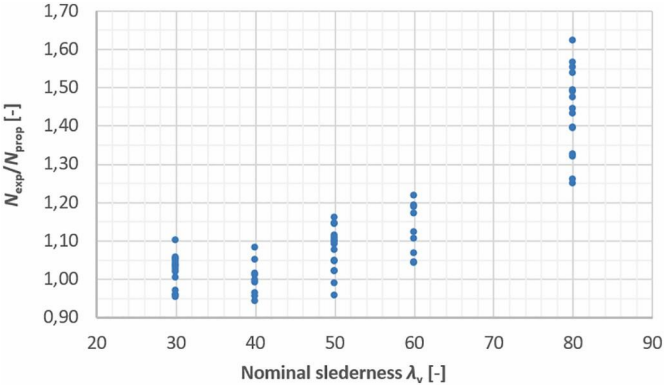

Fig. 14. Ratio between experimental and analytical load for the Tsinghua University tests

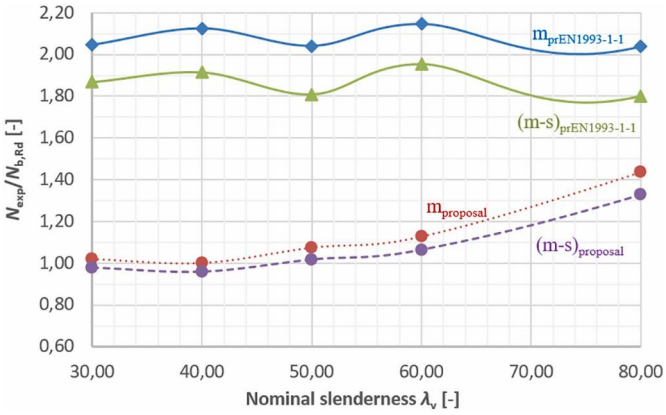

Fig. 15. Ratio between experimental and analytical loads for the Tsinghua University tests, mean values.

Table 8
Comparisons for the centrally loaded ULiège tests.

No	Specimen label	$\overline{\lambda_v}$ [−]	Class	$N_{exp}/N_{Rd,prEN1993-1-1}$ [−]	$N_{exp}/N_{Rd,prop}$ [−]
1	Sp11	1,31	1	1,13	1,13
2	Sp13	1,56	1	1,04	1,04
3	Sp15	1,81	1	1,04	1,04
4	Sp21	1,12	4	1,12	1,06
5	Sp23	1,30	4	1,02	0,99
6	Sp25	1,48	4	1,08	1,05

4.2. Angelhy compression tests at ULiège

At the University of Liege, 12 compression tests were carried out on axially loaded pin-ended columns with or without eccentricity in the frame of the ANGELHY project; they are reported in Ref. [17]. Amongst them, 6 were loaded at the centre of gravity and 6 at the point P_2, as this is illustrated in Fig. 8(b). The cross-sections were L 150x150x18 and L 200x200x16 with three different lengths. The material was high strength steel (HSS) S420 and S460. The load was introduced through supports that correspond to fully hinged boundary conditions, allowing free rotation in- and out-of-plane.

The ratio between the experimental load and the buckling resistance from prEN 1993-1-1 as well as the resistance determined by the current proposal (see section 2.1) of the tests without eccentricity, are reported in Table 8. As for

Published in : Journal of Constructional Steel Research (2022), vol. 189, 107092, pp. 1–15
DOI: 10. 1016/j.jcsr.2021.107092
Status : Postprint (Author's version)

all centrally loaded specimens, the first instability mode was a flexural one, the value for the non-dimensional slenderness is the same for both procedures. Therefore, the difference of the ratios reported in Table 8 are due to the way to incorporate local buckling, which differs in both procedures.
In Ref.[17], the conservative character of the general method for angle members was highlighted. In the following, the general method, as adapted for angles (see section 2.5), is applied for the eccentrically loaded specimens and compared with the provisions of prEN 1993-1-1. The results are summarized in Table 9; two cases (Case 1 and Case 3 as defined in section 3.5) were considered for the determination of the analytical load.

Table 9
Comparisons for the eccentrically loaded ULiege tests – general method.

No	Specimen label	$N_{exp}/N_{Rd,prEN1993-1-1}$ [–]	$N_{exp}/N_{prop,c1}$ [–]	$N_{exp}/N_{prop,c3}$ [–]
1	Sp12	1,88	1,46	1,11
2	Sp14	1,77	1,38	1,09
3	Sp16	1,72	1,33	1,10
4	Sp22	2,62	1,60	1,21
5	Sp24	2,41	1,47	1,14
6	Sp26	2,30	1,39	1,12

It may be seen that the analytical method provides less conservative and safe side predictions for all test subjected to compression and bending. It should be noted that the specimens Sp22, Sp24 and Sp26 are categorized in class 4 according to prEN 1993-1-1 and therefore the W_{eff} value is used for the determination of the maximum stress. In contrast, according to the current proposal, all the profiles reach at least their elastic resistance in bending and so the W_{el} value is used.

4.3. Eccentric compression tests at NTUA

At the National Technical University of Athens, 33 compression tests were carried out on axially loaded pin-ended columns with or without eccentricity and reported in Ref. [19]. The cross-sections were equal-leg angles L 70 × 70 × 7 and the material S275. The profile was classified by EN 1993-1-1 in class 1. The load was introduced through supports that correspond to spherical hinged boundary conditions. The experimental results are compared with the resistance formulae of the current proposal as outlined in section 2.4, as well as with the resistance formulae for members as described in prEN 1993-1-1, eqs. (8.88)–(8.89), in combinations with annex C where interaction factors for mono-symmetric sections are given.
Fig. 16 presents the ratio between the experimental resistances and the analytical ones obtained using current proposal (see section 2.4) versus the non-dimensional slenderness $\overline{\lambda_v}$, for all tests except one that its experimental load was higher than its critical one. Such a phenomenon was observed in similar angle tests of other Laboratories. It should be the result of very small geometrical imperfections, which are in opposite direction to those corresponding to the fundamental buckling mode that leads the angle tips to compression.
Fig. 17 presents the mean value (m) of the ratio between the experimental loads and the analytical loads as determined by the above methods, and the mean minus one standard deviation value (m-s). It can be seen that the current proposal gives a better prediction for the column capacity compared to the existing version of prEN 1993-1-1 and is always on the safe side.

Published in : Journal of Constructional Steel Research (2022), vol. 189, 107092, pp. 1–15
DOI: 10. 1016/j.jcsr.2021.107092
Status : Postprint (Author's version)

4.4. Eccentric compression tests at TU Graz

At the Technical University of Graz, 27 compression tests were carried out and reported in Ref. [11] on equal angle sections: 24 on L 80 × 80 × 8 and 3 on L 120x120x12 profiles. The material was S275 for all specimens. The boundary conditions varied from clamped supports (13 tests in series BC1), to knife supports allowing rotation in the loading plane (5 tests in series BC2) and fully hinged support allowing free rotation in- and out-of-plane (9 tests in series BC3). The load was introduced to the profile through one leg by the bolts; the introduction point is the centre of the hole for connection with one bolt (13 tests), or the centre between the two holes for connection with two bolts (14 tests).

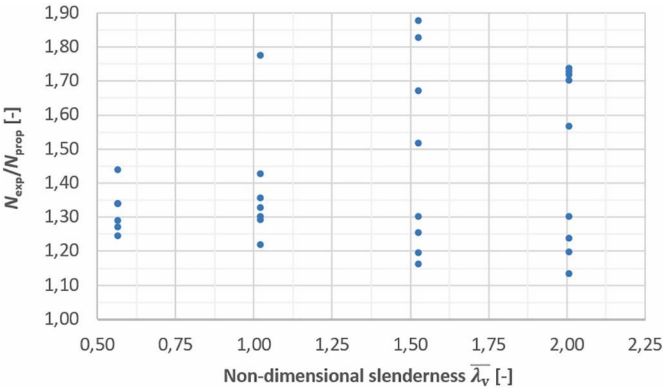

Fig. 16. Ratio between experimental and analytical loads for the NTUA tests.

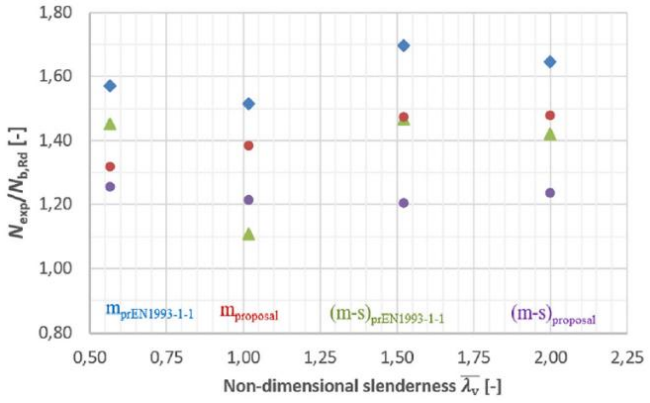

Fig. 17. Ratio between experimental and analytical loads for the NTUA tests, mean values.

For this experimental campaign, the member capacity was calculated firstly by the proposed method, checking the angle member to compression and biaxial bending that results from the loading eccentricity. The buckling length was set equal to the system length L_{sys} for all cases, except where both following conditions were met: support conditions BC1 and connection by two bolts; in the latter case, the buckling length was set equal to $L_{sys}/2$.
The results of the current proposal are compared with the provisions of EN 1993-3-1, Annex G and not the ones of prEN 1993-1-1 as before, so as to account for the effect of the bolted connection. In this case, the member is checked to compression through an effective slenderness that takes into account both the eccentric loading and the end restraints provided by the bolted connection. Buckling is checked in respect to the weak (v) and geometric (y) axes. The relevant effective slenderness is determined from the following equations (Table G.2 of EN 1993-3-1, Annex G):

Published in : Journal of Constructional Steel Research (2022), vol. 189, 107092, pp. 1–15
DOI: 10. 1016/j.jcsr.2021.107092
Status : Postprint (Author's version)

$$\bar{\lambda}_{eff,v} = 0{,}35 + 0{,}7 \bullet \bar{\lambda}_y \quad \text{for connection with 2 bolts} \qquad (27)$$

$$\bar{\lambda}_{eff,v} = \begin{cases} 0{,}40 + 0{,}7 \bullet \bar{\lambda}_y \\ 0{,}58 + 0{,}7 \bullet \bar{\lambda}_y \end{cases} \quad \text{for connection with 1 bolt} \qquad (28)$$

The design resistance, where $\chi = \min\{\chi_v, \chi_y\}$, may be obtained as follows:

$$N_{b,Rd} = \begin{cases} \dfrac{\chi A f_y}{\gamma_{M1}} & \text{for connection with 2 bolts} \\ 0{,}8 \cdot \dfrac{\chi A f_y}{\gamma_{M1}} & \text{for connection with 1 bolt} \end{cases} \qquad (29)$$

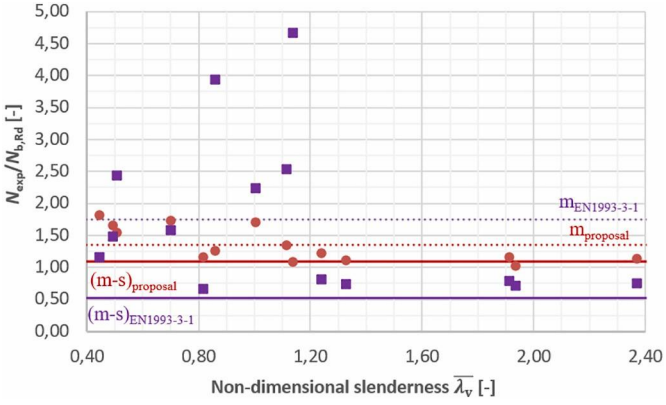

Fig. 18. Ratio between experimental and analytical loads for the TU Graz tests with two bolts.

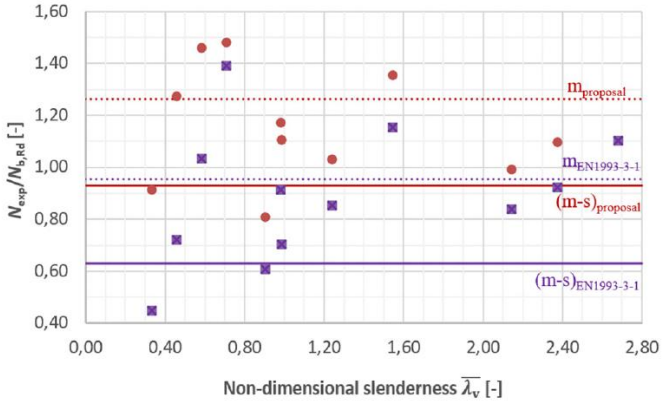

Fig. 19. Ratio between experimental and analytical loads for the TU Graz tests with one bolt.

The member resistance is the lowest between the resistances in respect to the v-v and y-y axes.

Figs. 18 and 19 illustrate the ratio between the experimental and the analytical loads for connection with two and correspondingly one bolt and provide the mean minus one standard deviation value for all tests. It may be seen that the proposed method provides safe predictions for all tests with two bolts, and all but 3 tests with one bolt. In contrast, the EN 1993-3-1 method largely overestimates the angle capacities and is on the unsafe side. The authors in Ref. [11] conclude that the existing EN 1993- 3-1 method for compression angles connected with one bolt is unsafe and that consequently they should be designed as simply supported members by 2nd order analysis accounting for

Published in : Journal of Constructional Steel Research (2022), vol. 189, 107092, pp. 1–15
DOI: 10. 1016/j.jcsr.2021.107092
Status : Postprint (Author's version)

geometrical imperfections in respect to the weak axis and subsequent cross-section check. This statement is confirmed by the present study.

4.5. Eccentric compression tests at TUBRaunschweig

At the Technical University of Braunschweig, 40 compression tests were carried out and reported in Ref. [20] on equal leg angle L 50x50x5 profiles. The specimen lengths were 300, 600, 900, 1200 and 1500 mm, while the material was S355. The end support conditions were defined by the authors in Ref. [20] as clamped and hinged. In the former the angle was connected with one preloaded bolt to a steel tab, in the latter through a pin to a fork bearing. The load was introduced through one bolt M12.
Fig. 20 presents, for all tests, the ratio between the experimental resistances and the analytical ones obtained using current proposal (see section 2.4) according to the weak axis non-dimensional slenderness λ_v. Fig. 21 presents the ratio (mean minus one standard deviation) of the experimental to analytical loads as a function of the relative weak axis slenderness.

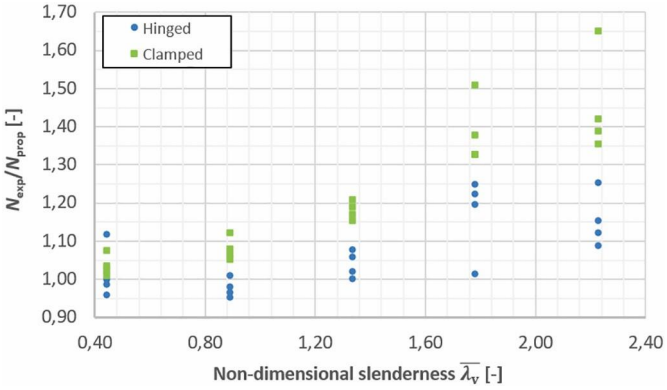

Fig. 20. Ratio between experimental and analytical loads for the TU Braunschweig tests.

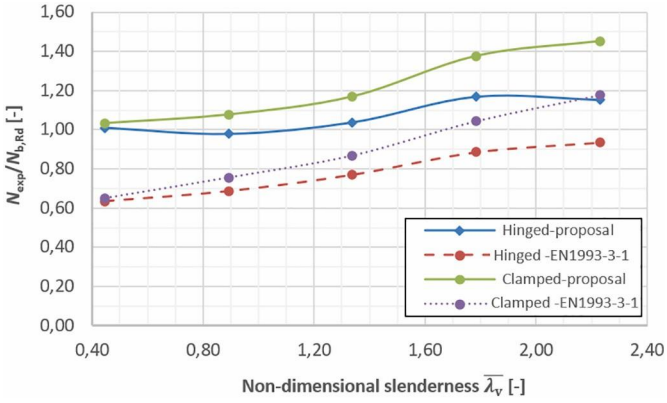

Fig. 21. Ratio of experimental to analytical loads as determined by the proposed method and the provisions of EN 1993-3-1, mean minus one standard deviation values.

Similarly to the previous section, the analytical load was determined either by the proposed method, under consideration of the moments that result from the loading eccentricity, or by the provisions of EN 1993-3-1. As in Ref. [20], the buckling length was set in all cases equal to the system length, even in the case of the "clamped" support conditions, due to the free rotation of the specimen around the one supporting bolt. This was a conservative

assumption since the bolts were preloaded and provided some rotation restraint. In fact, the experimental loads were up to 20% higher for the largest slenderness in the "clamped" support conditions. It may be seen that the proposed method gives best results for the hinged support conditions while for the clamped support seem to underestimate the buckling capacity at larger slenderness. In contrast, the provisions of EN 1993-3-1 appear to overestimate the capacity, especially for hinged support conditions. The conclusion of the authors in Ref. [20] is therefore confirmed that: "…. the simplified method of EN 1993-3-1 for the one screw joint in the existing form is not wise to be used in practice".

5. Conclusions

In the paper, a full set of design rules for members is provided which may directly lead to the revision of present existing Eurocode provisions. These rules are written in the Eurocode format and will be included in the forthcoming version of prEN 1993-1-1 in Annex F. Their main features are as follows:

- The rules are generic for the referred profiles and do not apply only for lattice towers.
- They are simple to apply and are derived from basic rules of the stability theory.
- They represent the mechanical behavior and failure modes of cross- sections and members.
- They account directly for the presence of applied moments resulting from the connection eccentricities.
- Appropriate European buckling curves for flexural and lateral torsional buckling of angles are proposed.

All the design rules were validated by extensive numerical analyses and numerous experimental tests. Experimental results were also compared to existing Code provisions. It was shown that the proposed method predicts well the member capacity and may be used as an alternative to existing Code provisions.

Declaration of Competing Interest

The authors declare that they have no known competing financial interests or personal relationships that could have appeared to influence the work reported in this paper.

Acknowledgments

The work presented here is carried in the framework of a European Research project entitled ANGELHY "Innovative solutions for design and strengthening of telecommunications and transmission lattice towers using large angles from high strength steel and hybrid techniques of angles with FRP strips", with a financial grant from the Research Fund for Coal and Steel (RFCS) of the European Community. Partners of the project were NTUA, ULiège, ArcelorMittal, CTICM, COSMOTE and SIKA France. The authors gratefully acknowledge this financial support.

REFERENCES

[1] EN 1993-1-1, Design of Steel Structures - Part 1–1: General Rules and Rules for Buildings, Comité Européen de Normalisation (CEN), Brussels, 2005.
[2] prEN 1993-1-1, Design of Steel Structures - Part 1–1: General Rules and Rules for Buildings, Comité Européen de Normalisation (CEN), Brussels, 2019.

[3] EN 1993-3-1, Design of Steel Structures - Part 3–1: Towers, Musts and Chimneys. Tower and Musts, Comité Européen de Normalisation (CEN), Brussels, 2005.
[4] EN 1993-1-8, Design of Steel Structures - Part 1–8: Design of Joints, Comité Européen de Normalisation (CEN), Brussels, 2005.
[5] EN 1993-1-5, Design of Steel Structures - Part 1–5: Plate Structural Elements, Comité 000.Europeen de Normalisation (CEN), Brussels, 2006.
[6] EN 50341-1, Overhead Electrical Lines Exceeding AC 1 kV - Part 1: General Requirements - Common Specifications, 2012.
[7] I. Vayas, J.P. Jaspart, A. Bureau, M. Tibolt, S. Reygner, M. Papavasiliou, Telecommunication and Transmission Lattice Towers from Angle Sections – the ANGELHY Project, doi:10.1002/cepa, Ernst & Sohn, ce/papers, Special Issue: EUROSTEEL 2021 Sheffield — Steel's coming home 4 (2–4) (2021) 210–217.
[8] Load and resistance factor specifications for single-angle members, AISC (2000).
[9] Design of Latticed Steel Transmission Structures, ASCE/SEI 10–15, 2015.
[10] N. Schillo, M. Feldmann, Buckling resistance of L-profiles in towers, masts and open line constructions, Stahlbau 84, Heft 12 (2015) 946–954.
[11] M. Kettler, H. Unterweger, Laboratory tests on bolted steel angles in compression with varying end support conditions, Stahlbau 88 (H5) (2019) 447–459.
[12] A. Hussain, Y.P. Liu, S.L. Chan, Finite element modelling and design of single angle member under bi-axial bending, Structures 16 (2018) 373–389.
[13] P.B. Dinis, D. Camotim, A novel DSM-based approach for the rational design of fixed-ended and pin-ended short-to-intermediate thin-walled angle columns, Thin- Walled Struct. 87 (2015) 158–182.
[14] P.B. Dinis, D. Camotim, Proposal to improve the DSM design of cold-formed steel angle columns: need, background, quality assessment and illustration, J. Struct. Eng. ASCE 145 (8) (2019) paper 04019071.
[15] P.B. Dinis, K.G. Santana, A. Landesmann, D. Camotim, Numerical and experimental study on CFS spherically-hinged equal-leg angle columns: stability, strength and DSM design, Thin-Walled Struct. 161 (2021) paper 106862.
[16] P.B. Dinis, D. Camotim, A. Landesmann, Design of simply supported hot-rolled steel short-to-intermediate angle columns – design approach based on the direct strength method (DSM), Steel Construct. 12 (4) (2019) 278–290.
[17] M.Z. Bezas, J.F. Demonceau, I. Vayas, J.P. Jaspart, Experimental and numerical investigations on large angle high strength steel columns, Thin-Walled Struct. 159C (2021) 107287, https://doi.org/10.1016/j.tws.2020.107287.
[18] H.Y. Ban, G. Shi, Y.J. Shi, Y.Q. Wang, Column buckling tests of 420MPa high strength steel single equal angles, Int. J. Struct. Stab. Dyn. 13 (2) (2013), pp. 1250069-1–1250069-23.
[19] A. Spiliopoulos, M.E. Dasiou, P. Thanopoulos, I. Vayas, Experimental tests on members made from rolled angle sections, Steel Construct. Design Res. 11 (1) (2018) 84–93.
[20] M. Reininghaus, M. Skottke, Dimensioning of pressed angle steel with one screw joint based on the standards DIN 18800-2 and EN 1993-3-1, Stahlbau 74 H7 (2005) p.p.534-538.
[21] Innovative Solutions for Design and Strengthening of Telecommunications and Transmission Lattice Towers using Large Angles from High Strength Steel and Hybrid Techniques of Angles with FRP strips, Grant Agreement number: 753993 — ANGELHY — RFCS-2016/RFCS-2016, 2016.
[22] prEN 1993-3, Design of Steel Structures - Part 3: Towers, Musts and Chimneys, Comité Européen de Normalisation (CEN), Brussels, 2021.
[23] M.Z. Bezas, J.F. Demonceau, I. Vayas, J.P. Jaspart, Classification and cross-section resistance of equal-leg rolled angle profiles, J. Constr. Steel Res. 185 (2021), 106842, https://doi.org/10.1016/j.jcsr.2021.106842.
[24] B. Behzadi-Sofiani, L. Gardner, M.A. Wadee, P.B. Dinis, D. Camotim, Behaviour and design of fixed-ended steel equal-leg angle section columns, J. Constr. Steel Res. 182 (2021) paper 106649.
[25] D. Camotim, P.B. Dinis, A. Landesmann, Behavior, failure and direct strength method design of steel angle columns: geometrical simplicity versus structural complexity, J. Struct. Eng. ASCE 146 (11) (2020) paper 04020226.
[26] M.-Z. Bezas, Design of Lattice Towers from Hot-Rolled Equal Leg Steel Angles, PhD thesis, http://hdl.handle.net/2268/262364.
[27] R. Greiner, A. Lechner, M. Kettler, J.P. Jaspart, K. Weynand, R. Oerder, V. Dehan, Valorisation Action of Plastic Member Capacity of Semi-Compact Steel Sections: A more Economic Design (SEMI-COMP+), RFCS European Research Project, Directorate-General for Research and Innovation (European Commission), 2013. ISBN 978-92-79-29312-2.

Published in : Journal of Constructional Steel Research (2022), vol. 189, 107092, pp. 1–15
DOI: 10. 1016/j.jcsr.2021.107092
Status : Postprint (Author's version)

[28] I. Vayas, A. Charalampakis, V. Koumousis, Inelastic resistance of angle sections subjected to biaxial bending and normal forces, Steel Construct. 2 (2) (2009) 138–146.
[29] ABAQUS, User's manual, Version 6.14, Simulia, 2014.
[30] Y. Shifferaw, B.W. Schafer, Cold-formed steel lipped and plain angle columns with fixed ends, Thin-Walled Struct. 80 (2014) 142–152.
[31] EN 1090-2, Technical Requirements for the Execution of Steel Structures, Comité Européen de Normalisation (CEN), 2008.
[32] prEN 1993-1-14, Design of Steel Structures - Part 1–14: Design Assisted by Finite Element Analysis, 2018.
[33] L. Zhang, J.P. Jaspart, Stability of Members in Compression Made of Large Hot- Rolled and Welded Angles, Research Report, University of Liège, 2013.
[34] P. Moze, L.G. Cajot, F. Sinur, K. Rejec, D. Beg, Residual stress distribution of large steel equal leg angles, Eng. Struct. 71 (2014) 35–47.
[35] FINELG, Non-linear Finite Element Analysis Program, User's Manual, Version 9.0, Greisch Ingeniere, 2003.